Journal of Applied Botany and Food Quality 97, 102 - 114 (2024), DOI:10.5073/JABFQ.2024.097.013

[1]Food Security and Public Health Department, Khabat Technical Institute, Erbil Polytechnic University, Erbil, Iraq
[2]Harran University, Engineering Faculty, Food Engineering Department, Şanlıurfa, Turkey

Starch and green silver nanoparticles based functional nanocomposite films: New insights in fresh fruit packaging

Bakhan Mohammed Rustum[1], Bülent Başyiğit[2], Mehmet Karaaslan[2*]

(Submitted: April 1, 2024; Accepted: June 15, 2024)

Summary

This study uses sour cherries (*Prunes census* L.*)* pomace extract as a reducing agent to demonstrate the creation of silver nanoparticles (AgNPs) and preparation of starch film via blending glycerol, polyethylene glycol, and produced starch-AgNPs in different concentrations 1, 2, 3, and 4% of AgNPs with starch film as control. The prepared starch-Ag nanocomposite films were used for packaging strawberries at 4 °C. Characteristics of the composite films included FTIR, XRD, SEM, and UV-vis spectroscopy. The composite films with 4% AgNPs showed a smooth surface, as the SEM results showed. Following blending with glycerol and AgNPs, the FTIR result changed the starch's structure. After adding AgNPs, the composite film s flexibility improved. The starch-Ag nanocomposite films demonstrated significant antimicrobial activity against *Staphylococcus aureus*, *Escherichia coli*, and *Candida albicans*. Weight loss was used to assess the impact of packing on the quality and shelf life of packed strawberries during storage, the effect time on pH, and microbial growth throughout a 14-day storage period. The results indicate that strawberry fruits may be kept fresher longer and their shelf life preserved with a 3% AgNPs starch-Ag nanocomposite. This is the first research that uses pulp extract from *Prunus census* L. to describe the production of AgNPs.

Keywords: Green silver nanoparticle, sour cherry, starch nanocomposite, and strawberry

Introduction

In recent years, greener synthetic approaches have piqued scientists' interest in synthesizing nanostructures on the micro-scale (Alam, 2022). Silver (Ag) nanoparticles (AgNPs) are a type of metal nanoparticles that are approximately 1-100 nm in length (Duncan, 2011; Alam, 2022) and may be employed as an antibacterial agent in food packaging to stop microbiological and foodborne illnesses (Herrera-Marín et al., 2023). They have been shown to suppress microorganisms' growth and survival, including pathogens like *Salmonella typhi, Escherichia coli,* or *Staphylococcus aureus* (Sheikh et al., 2022). Green nanoparticle synthesis is preferred over microorganisms due to their simplicity, ease of scale, and large concentrations, making them ideal for large-scale synthesis (Vinodhini et al., 2022). The use of plant extracts to reduce silver ions to silver nanoparticles has grown in popularity, developing new environmentally friendly methods of this field without needing expensive chemical reagents or equipment and following green chemistry (Herrera-Marín et al., 2023; Phuong et al., 2023; Wasilewska et al., 2023).

Nanocomposite films are used in food packaging to keep food safe, reduce chemical additives, and improve heat resistance. It is also gaining popularity due to its lower environmental impact. Starch, polypeptides, hyaluronic acid, sodium alginate, and heparin have all been used to produce green nanoparticles (Mohseni et al., 2020). Starch films offer numerous potential advantages because they have better mechanical and barrier qualities (Mao et al., 2023); however, starch-based foams have restricted applications due to their innate hydrophilicity and poor mechanical performance. Various additives have been introduced, considering starch foams' shortcomings (Tacha et al., 2023). Natural polymers and chemical substances like chitosan can be used in active packaging with antimicrobial properties for various food safety applications when combined with polysaccharide clay nanocomposites (Qu and Luo, 2021). Due to the low biodegradability and environmental impact of mass-produced discarded plastics (De Matteis et al., 2023), scientists have been working to produce newer polymers with greater environmental readability, particularly in food packaging.

Edible film and coatings extend fruit's off-shelf life and maintain food quality by avoiding alterations in flavo , texture, appearance, and aroma due to the prevention of respiratory gases and water vapor (Gol et al., 2013). The sour cherry (*Prunus census* L.) is also known as the tart cherry, a Rosaceae fruit (van de Klashorst et al., 2020; Yildiz et al., 2022). Turkey is the second largest sour cherry producer in the world (Başyiğit et al., 2020; Yildiz et al., 2022); cherries are affordable dietary antioxidants (Başyiğit et al., 2020), crucial for tumor cell regulation and preventing chronic diseases (Hurtado-Barroso et al., 2020; Fonseca et al., 2021). They are used in fresh, frozen, and processed nutraceutical products (Sheikh et al., 2022). Health benefits are most likely related to the presence of polyphenols and enrichment in anthocyanins (van de Klashorst et al., 2020), which are typically present in the fruit's skin and bear accountability for the fruit's rich red pigment (Khoo et al., 2017). Yildiz et al. (2022) examined the effects of heating, boiling, and microwave application on sour cherry juices. Results showed no significant differences in color values, anthocyanin content, intensity, or antioxidant activity. However, microwave application significantly increased phenolic substance concentrations, resulting in higher food safety. Even though, at standard serving sizes, they have one of the highest capacities of any fruit to absorb oxygen radicals (van de Klashorst et al., 2020).

This study's objective is to create AgNPs out of a fluid mixture of sour cherry waste extract, and $AgNO_3$ solution to produce a composite thin film to protect strawberry fruit and extend its shelf life, preserve the valuable metabolites such as polyphenols and other phytochemicals (Donno et al., 2013).

Materials and methods

Materials

Fresh sour cherries were provided at the neighborhood market in Kutahya, Turkey. Yildiz et al. (2022) reported that fruit waste extracts prepared from sour cherry juice production were used to synthesize

* Corresponding author

nanostructures after making sour cherry juice. The fruit wastes were kept in polypropylene bags at 25 °C for 30 d without sunlight. This study made use of sodium hydroxide (NaOH), silver nitrate ($AgNO_3$) manufactured by (Merck, Darmstadt, Germany), hydrochloric acid, sodium hypochlorite, starch soluble (extra pure) (Biochem Chemopharma, Cosne-Cours-sur-Loire, France), polyethylene glycol (Biochem), and glycerol (Biochem). Throughout the investigation, double distilled water was used. Chemicals used throughout the study were used from Merck unless otherwise stated.

Green synthesis of silver nanoparticles from Sour cherry waste extract

The ecosynthesis of metal oxide (MO) and bioactive metal (M) nanostructures (NSs) was using a portion of food, food waste, and plant extracts for the creation of the functionalized M NPs and MO NPs without the use of toxic, hazardous, or harmful ingredients. Initially, 90 ml of double distilled water was mixed with 1.0 g of powdered sour cherries. The mixture was then submerged in a water bath at 60 °C for 20 min. Whatman filter paper was then used to filter the mixture, and the extract (filtrate) was stored at 4 °C.

The ecosynthesis of AgNPs was carried out based on Suman et al. (2013) and Ali et al. (2022). The waste extract solution was mixed with an aqueous solution of $AgNO_3$ (1.0 M) (1:9) ratios (best effect) at pH 8 (Mohseni et al., 2020). The solution was then swirled on a heating stirrer until its color changed because surface Plasmon vibrations in AgNPs are excited; they appear yellowish brown in aqueous solution (Suman et al., 2013). It was eventually covered with aluminum foil to prevent oxidation. The creation and characterization of AgNPs were examined by temperature, pH, and time for the optimum reaction extraction.

Optimization of AgNPs

The solutions were centrifuged at 5000 rpm and dried for identification. Skiba et al. (2020) employed an optimization approach in the green synthesis of AgNPs. A spectrophotometer (Varian, Cary 100 Cone model, U.S.A.) with a 350-550 nm range was used to record the AgNPs UV-vis transmission spectra. The impacts of different temperatures of 40-85 °C, time 10-60 min, and pH 6-9 on the creation of nanoparticles were explored for synthesizing (20) different AgNPs.

Synthesis of starch film

According to the process employed by Teodoro et al. (2015), corn starch has been produced with a few adjustments. In order to create a homogenous solution, the maize starch (4.0 g) is spread out in 100 ml water and then stirred by a heater for 20 min. They were added to the starch solution after combining polyethylene glycol and glycerol at a 2:0.4 ratio. To create the films, pour 15 ml of the solution onto a Petri dish with a 14 cm diameter after chilling in known quantities after spending 15 min in a hot water bath. A thin starch film is obtained after 24 h of drying at 62 °C in the oven. A thin film, a nanocomposite, was obtained and used in packing food.

Synthesis of starch-AgNPs nanocomposite film

Adding AgNPs, as reported by Suman et al. (2013), at the ratios 1, 2, 3, and 4% (1 to 4 ml AgNP solution, v/v) in 100 ml into (starch film) solution to provide starch-Ag-nanocomposite is due to incorporating appropriate ratios of AgNPs into the film mechanical characteristics, and physical resistance is increased.

Characterization of AgNPs and starch-Ag nanocomposite

Scanning Electron Microscope (SEM) images, the Transmission spectrum of the Fourier transform infrared (FTIR), and evaluations using X-ray diffraction (XRD) spectroscopy were conducted by earlier research (Başyiğit et al., 2022). A Thermos Nicolet spectrometer (Nexus 870, USA) was used to produce the Transmission spectrum of the Fourier transform infrared (FTIR) of the sour cherry waste extract and AgNPs in the 4000 to 400 cm^{-1} KBr disk transmission mode. The usage of X-ray diffraction (XRD) obtained the AgNPs spectra using a diffractometer by scanning the samples across a 20 range of 5-60° under a continuous scan at a step size of 0.02 using Shimadzu XRD-6000 (Shimadzu, Tokyo, Japan), and then using a Zeiss Sigma 300 SEM for field emission (Oberkochem, Germany). Both the size and morphology of the starch-nanocomposite film and AgNPs were examined.

Physicochemical characteristics of thin film

Moisture content

The moisture content of the blend films was determined by calculating the loss-weight of edible films that were preconditioned and dried in an oven at 105 ± 1 °C for 24 h (Kumar et al., 2020).

$$MC = \frac{M1 - M2}{M1} \times 100$$

Thickness

A digital micrometer (Q.L.R. digit-IP54, China) was used to measure the thickness of each blend film at ten randomly selected sites with an accuracy of 0.001 mm. Other calculations used average values (Pirsa et al., 2020).

Color parameters

The color values of composite film samples were evaluated using a colorimeter (D25-9000, Hunterlab, U.S.). After locating edible film samples on a white standard plate with L*=95.49, a*=-0.30, and b*=-0.08, the films brightness, redness-greenness, and yellowness-blueness values were calculated. Equation (~E) was used to measure the overall color difference (Omar-Aziz et al., 2021).

$$\Delta E = \sqrt{[(L - L^*)2 + (a - a^*)2 + (b - b^*)2]}$$

AgNP antimicrobial activity using the Agar diffusion method

Agar well diffusion techniques were used based on Abdollahzadeh et al. (2021), with some modifications to measure the AgNPs' antimicrobial activity against Gram-positive (*S. aureus*) and Gram-negative (*E. coli)* bacteria and *C. albicans* as fungal microorganisms. Before testing, the pathogenic bacteria (*S. aureus*) and (*E. coli*) were aseptically cultivated at 37 °C for 16 hr in trypticase soy agar (TSA) and brain-heart infusion (BHI) broth medium. After serially diluting each bacterial culture in 0.1 mL of sterilized (D.W.). 100 mL of TSA and BHI agar media were mixed with 1 mL (1,49 × 10^6 CFU/mL) of cells from diluted broths before plating, and 6 mm-diameter agar wells were drilled into the media to create the wells. The wells were filled with sample solutions (80 µL) and incubated at 37 °C for 24 h. The inhibition zone diameter (mm) of the microbial growth around the wells was measured to estimate the method (Rhim et al., 2013), all tests were for nanocomposite film s antibacterial efficacy using agar diffusion assay. Remel, Lenexa, Kansas, offers a Muller-Hinton agar (MHA) medium streaked in individual cultures of *S. aureus*, *E. coli*, and *C. albicans* to guarantee improved antimicrobial disk diffusion. The four different starch-Ag nanocomposite films containing 1, 2, 3, and 4% AgNPs were cut into circular discs with 5 mm diameters. The MHA medium will be topped with one circular disc from each film, and the plates will then be cultured at 37 °C for 24 h with pathogenic bacteria. A film sans AgNPs (starch-thin film) is used as a control. The inhibitory zone diameters will be calculated by deducing the diameter of the disc from the diameter of the inhibition zone as a whole (mm). However, potato dextrose agar (PDA) was used for mold and yeast tests on strawberry-coated fruits.

DPPH radical scavenging activity

Antioxidant activity utilizing a modified version of the extraction procedure published by YANG et al. (2023), the produced films antioxidant activity was evaluated. The film samples (0.1g) were agitated in a 24-h shaker without exposure to light after being combined with a 50% ethanol solution (5 ml). The combined solution was then centrifuged. A centrifuge tube containing 1 mL of supernatant and, for an h, 2 ml of 0.1 mg DPPH (1, 1-diphenyl-2-picrylhydrazyl) ethanol solution was stored in the dark for 10 min. The capacity was measured with a fluorescence microplate reader (Biotek, USA). DPPH radical scavenging rate (%) was calculated as follows:

DPPH radical scavenging activity (%) = (A control-A sample)/100

Nanocomposite coating

In Erbil, Iraq, strawberries were purchased in a neighborhood market. The same color, size, fungal decay, and lack of physical damage were used to choose the fruits (WIGATI et al., 2023). Fruits were washed with 1% (v/v) sodium hypochlorite for 1 min and rinsed with distilled water. Then, samples were dried for 2 h at room temperature by using lint-free tissue. Coating solutions were made using glycerol as a plasticizer and a starch-Ag nanocomposite. Before being used, the solution was shaken for 15 min at room temperature. Samples were coated by soaking as outlined by WIGATI et al. (2023) with some modifications. Strawberry fruit was washed and air dried for 2 h at room temperature after being surface cleaned for 2 min in a 2% sodium hypochlorite solution. Each treatment consisted of three repetitions and 24 fruits divided among four groups according to randomization. Each of the five coating treatments (S1, 2, 3, and 4 is present 1, 2, 3, and 4% AgNPs in starch-Ag nanocomposite film, and S5 is starch nanocomposite (starch film), was given to one of five groups. The fruit in the sixth group, known as control or uncoated (S6), was untreated and dipped in distilled water. The samples were kept at 4 °C and 70-75% relative humidity (RH) in plastic containers. Quality characteristics and the enzyme activities were assessed at the start of the experiment at (0 d) and after 72 h, 1 week, 10 d, and 14 d of storage. Data for uncoated (control) fruits were only collected for the first 2 d of storage since, after that point, the fruit started to deteriorate (GOL et al., 2013).

Storage analysis for the coated foods

A digital balance (0.01 g) model TE12025 (Sartorius, Canada) was used to measure the weight of the strawberries. According to the AOAC (1994) standard technique, the weight loss percentage of strawberries was ascertained by weighing samples (72 fruits per replication) both at the beginning (i.e., day 0) and the end of each storage period in comparison to their initial weight. The results were reported as % weight reduction. Deterioration in strawberries was characterized as an apparent infection with grey mold, brown patches, or the injured region becoming softer (SHANKAR et al., 2021). According to the AOAC (1994) standard procedure, the fruit samples pH was measured using a digital pH meter (HANNA, Holand model: ELICO, LI120) (SAMBUCETTI and ZULETA, 1996; GOL et al., 2013).

Statistical analysis

A triple of each measurement was made unless otherwise noted. The mean± SD is the reported value for the experimental data. Data was analyzed using the statistical program SPSS (SPSS 23.0, I.B.M., Armonk, NY, USA). One-way analysis of variance (ANOVA) was used in the statistical analysis, along with Duncan's multiple range test as a post-hoc test, at a 95% confidence level ($p < 0.05$).

Results and discussion

Green synthesis of silver nanoparticles from Sour cherry waste extracts

Spectroscopic and analytical techniques are used for nanoparticle characterization, including silver nanoparticles, concentrating on their morphology, elemental composition, distribution, stability, and nature, as SHEIKH et al. (2022) reported.

Optimization of AgNPs

The production of AgNPs was validated by the color change from white to yellow, intense brown; As presented in the Fig. 1, the color shift in the ($AgNO_3$) mixture to brown shows the creation of AgNPs. The UV-Vis spectra show a prominent surface plasmon resonance (SPR) band at 400-450 nm, which verifies the production of AgNPs. The AgNPs produced during plasma-chemical synthesis were centrifuged at 5000 rpm for 5 min (SKIBA et al., 2020); as a result of silver ion reduction and surface plasmon resonance in an extraction combination of plant extracts with silver nitrate at room temperature; it was noticed within a 30 s of exposure to sunlight (MOHSENI et al., 2020). Among 20 synthesized AgNPs, a maximum clear peak has been shown at 462, 458, 456, 451, and 435 nm for samples (S20, S17, S2, S16, and S14), respectively, as shown in Fig. 2, whereas there was no peak visible in the sour cherry extract UV-vis spectrum. The nanoparticle size distribution was found to be 58 nm. Overall, the literature states that pure silver should exhibit absorption bands above 390 nm, and the production of AgNPs revealed a distinct peak at a wavelength between 400 and 500 nm (SEEKONDA and RANI, 2022; TACHA et al., 2023; WASILEWSKA et al., 2023). Effects of temperature, pH, and stirring time on the AgNPs and U.V.U.V. spectra of the $AgNO_3$-plant extract are displayed. The optimal temperature for extraction was determined to be 62 °C because, as shown in Fig. 2, the absorption increased as the temperature rose from 40 to 62 °C and subsequently dropped to 75 °C. Due to the $AgNO_3$ solution's pH value, the synthesis of AgNPs is significantly affected by pH, as shown in Fig. 3. The synthesis showed that pH 6.6 had a larger absorption value than other pH values. Hence, it was selected for the synthesis. According to WASILEWSKA et al. (2023), unique particles with varying antibacterial activity were found in each extract, which had a pH range of 2.1 to 6.2. However, the sour cherry extract was well chosen to produce NPs. Since the reaction absorption value was higher after 10 min of reaction time than at other times. Plasma therapy for 1 to 6 min reduces absorption strength, while gradually decreasing the concentration of silver ions in the solution. A comparable phenomenon presumably relates to transforming silver nanoparticles to silver oxide nanoparticles without a stabilizing reagent (SKIBA et al., 2020). SHEIKH et al. (2022) reported that a timing-related analysis of spectral UV-vis absorption data for AgNPs revealed a peak biosynthesis after 24 h, with the absorption peak rising over time, as

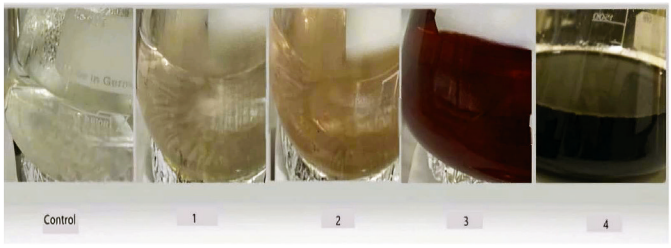

Fig. 1: Color change during reaction (control): $AgNO_3$ solution, (1): color changed by adding a few drops of plant extract after (5) min, (2): color changed by adding plant extract to the solution after (10) min, (3): color changed by adding plant extract to the solution after (20) min, (4): color changed with adjusting pH of solution its color indicates that AgNPs sensitized.

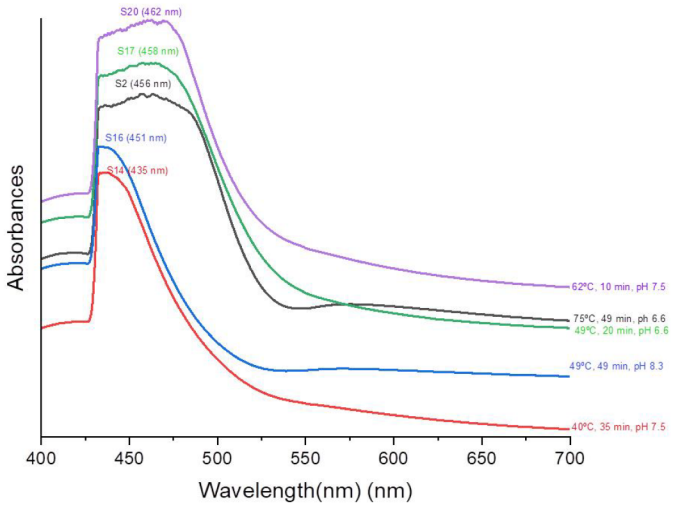

Fig. 2: Optimization of temperature, pH, and time reaction of $AgNO_3$-plant extract on UV-Vis's spectra.

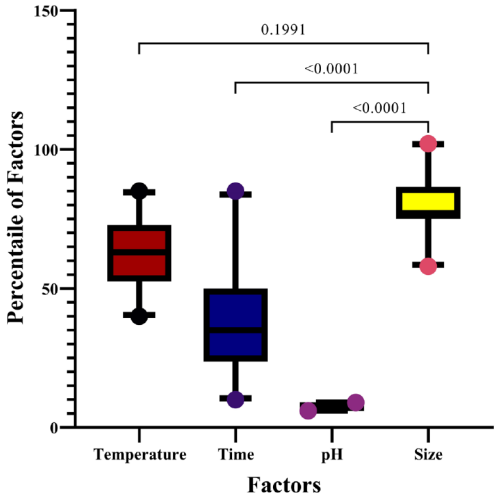

Fig. 3: Analysis of the effect of temperature, pH, and time reaction of $AgNO_3$-plant extract on UV-Vis's spectra.

shown in Fig. 2. In addition to improving barriers, nano clays /can reduce U.V.U.V. radiation by reflection or absorption, due to its enormous aspect ratio and surface area, the results of this study agree with (Qu and Luo, 2021), while do not agree with Skiba et al. (2020) were studied optimization process in green synthesis AgNPs. They reported that the optimum pH for green synthesis was (7-10) within 1-5 min. During the incubation of the ellagic acid-Ag^+ complexes, reaction temperature served as a driving factor, promoting electron transfer from ellagic acid to Ag+ and the formation of zero-valent Ag0 for the production of AgNPs (Ekrikaya et al., 2021). Demirbas et al. identified comparable pathways for NP creation. Anthocyanins in red cabbage extracts preferentially bind to Au3+ ions, forming anthocyanin- Au3+ complexes. Charge transfer from anthocyanin to Au3+ leads to the synthesis of Au+Cl2-, zero-valent Au0, and AuNPs (Demirbas et al., 2019).

Characterization of AgNPs and Starch-Ag nanocomposite film

The study used FTIR Fourier transform infrared, the reduction of Ag+ ions to silver oxide (AgO), capping, and stabilization of biosynthesized AgNPs as shown in the study of extracts and silver nanoparticles to examine the functional group in sour cherry extract (Alam, 2022). The FTIR spectra revealed multiple main bands, exhibiting notable peaks in the wavelength regions for the absorption. The study compared the functional groups in pure starch film with AgNPs in bioactive films and sour cherry extract with AgNPs from fresh and powder waste. As shown in Fig. 4, the FTIR spectrum of the sour cherry extract was obtained at various positions, including 3400.50 cm^{-1} and 2927.94, which indicates the presence of O-H and C-H stretching, respectively. 1734.01 cm^{-1} which is due to the presence of various carbonyl groups from carbohydrates proanthocyanins, hydroxycinnamic, hydroxybenzoic acids, gallotannins, ellagitannins, flavonols, anthocyanin flavanols', and other compounds were detected by N-O stretching 893.04 cm^{-1}, and C-H stretching in the range of 800-1500 cm^{-1} (Alam, 2022; Ali et al., 2022). Fig. 4 (a) shows the FTIR spectrum of freshly extracted *Prunus census* L. pomace-based manufactured AgNPs. The produced AgNPs' FTIR spectra show the presence of significant peaks at 2927.94 cm^{-1} is attributed to the aromatic compounds' C-H stretching as well as to the C-H functional groups, as well as to aromatic alkenes' C=C stretching at 1616 cm^{-1}, and C-O stretching at 1383 cm^{-1}. The vibratory stretching of the (N-H) C-O group is attributed to a weaker band at 1616 cm^{-1}.

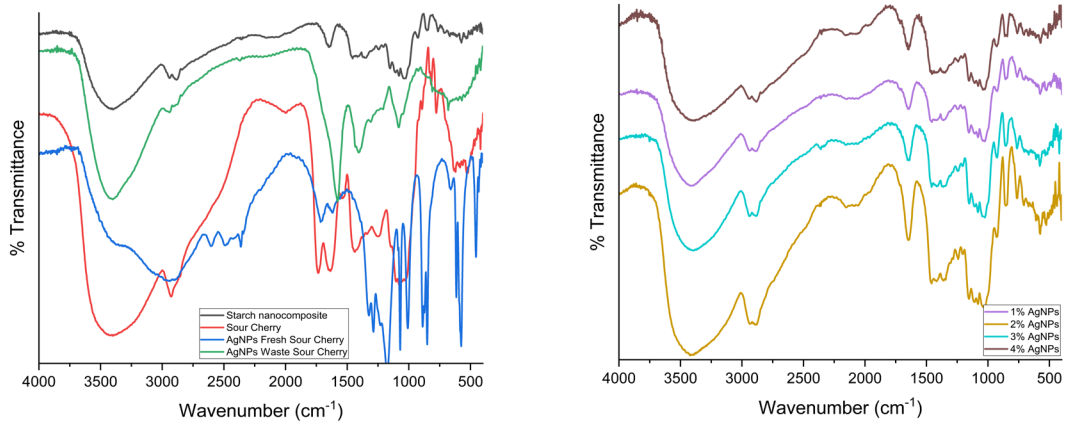

Fig. 4: **(a)** FTIR spectrum of synthesized AgNPs after reaction of the mixed solution of $AgNO_3$ and sour cherry pulp extract, **(b)** FTIR spectrum of synthesized starch-Ag nanocomposite biofilm with di ferent concentrations of AgNPs.

The spectrum shows two distinct and powerful absorption bands at 1070.49 cm^{-1} and 873.75 cm^{-1}, which are brought about by extending the vibration of stretched C=O coupled with C-H bending mode. Peaks at 873.75 cm^{-1} and 659.66 cm^{-1} demonstrate that AgNPs creation is not visible in sour cherry extract FTIR spectra (Ali et al., 2022). For the production of AgNPs, phytochemicals visible at infrared wavelength serve as agents that reduce or cap. Then, using qualitative testing, such phytochemicals discovered aqueous extracts included to pinpoint the biochemically active substances by examining the changing color (Alam, 2022). Standard biochemical procedures were used to identify these biochemical substances, containing tannin, coumarins, flavonoids, saponins, volatile oils, phenols, and sterols, as reported in Farnsworth (1966). While the absorption peaks in the FTIR spectrum of AgNPs made from waste powder occur at various locations, including 2939.52 cm^{-1} stretching of aromatic C-H, 1406.11 cm^{-1} for C-H stretching in aromatic alkene, and 1207.07 cm^{-1} for the stretching N-O bond, as well as C-O stretching, they are all related to the stretching of the aromatic chain as shown in Fig. 4 (a). Most starch nanocomposite comprises amylopectin and amylose, including the C-O-C and O.H.O.H. group and the CH2 and C.H.C.H. backbone. Each spectrum showed the presence of bonds at 3414, 3400, 3381, and 3367 cm^{-1} for O.H.O.H. stretching, 2939, 2885 cm^{-1} for C-H, and CH2 stretching respectively, 1463 cm^{-1} for CH3 symmetrical vibration (Mao et al., 2023). There is water present, as evidenced by the peaks at 1645 cm^{-1}. The bands' intensities differ at 3414, 3381, 3367, and 1107 cm^{-1} before and after the starch nanocomposite and $AgNO_3$ reaction. In starch-Ag nanocomposite as presented in Fig. 4 (b) with 1% AgNPs, the band's intensity at 3398, 3371, 3360, and1153 cm^{-1}, the vibration of O.H.O.H. groups connected to intra and inter-molecule hydrogen bonds in starch, water, and glycerol in the nanocomposite film. In the composite films FTIR spectra, multiple unique peaks at 1742 and 1600-1400 cm^{-1} were seen in all different starch-Ag nanocomposite films. The spectrometer identifies the absorbed wavelengths and produces an FTIR spectrum, a unique fingerprint of the chemical bonds in the material. Identifying chemical conjugation: In the case of chemically coupled AgNPs, the FTIR spectra of the starch-based film should exhibit modifications or shifts in the typical absorption bands associated with the starch molecules. These modifications may include position or intensity shifts in the starch polymers C-O, C-H, or O-H stretching vibrations. The appearance of new peaks or bands indicates the establishment of new chemical bonds between the AgNPs and the starch functional groups (e.g., hydroxyl, carbonyl, or ether groups). Chemically conjugated AgNPs cause changes in hydrogen bonding patterns within the starch matrix.

These findings indicated that the interaction between starch and AgNPs was done successfully because of Tween 80's C-O linkages and carvacrol's aromatic ring (Arrieta et al., 2013). The starch films hydroxyl peak was narrow and smaller when 4% AgNPs were present. Hydrogen bonding decreased the starch's free hydroxyl group and reduced the film s hydrophilicity, which is responsible for this outcome (Mao et al., 2023). The new interaction between the OH group in starch and $AgNO_3$ that results in the creation of OH-$AgNO_3$ can denote this reduction. Additionally, starch has several actives OH- groups that can interact with integrated Ag^+ ions through steric entrapment and chemical interactions. Ag^+ becomes involved with the polymer layer due to these interactions between the starch layer and Ag^+. Therefore, it is crucial to consider the possibility of producing silver nanoparticles due to the in-situ conversion of Ag^+ to their state of metallic (Taha et al., 2022). In this study (10 ml), aqueous $AgNO_3$ (1 µM) was used. The final concentration of AgNPs in the film might be 2.86 mg of Ag per kg dried film (ppm) depending on a study by (Ortega et al., 2017), which reported that the final concentration of AgNPs in the film was measured 28.6 mg of Ag per kg dried film (ppm) when (10 ml) aqueous solution of $AgNO_3$ (10 µM) used to produce starch nanocomposite films containing green AgNPs. Also, (Ferdous and Nemmar, 2020) reported that AgNPs in doses less than 10 mg/kg are safe, while AgNPs in doses more than 20 mg/kg are toxic. Fig. 5 shows the patterns of XRD for the synthesized AgNPs from silver nitrate and *P. census* L. Utilizing XRD, the crystalline structure for nanoparticles was examined. A small quantity of dry powder was used for the measurement, and they were deposited in the center of the XRD goniometer, which attached the nylon loop with a very viscous lubricant.

In the diffractogram of the AgNPs, five different peaks at angles of 2θ 26.410, 33.679. 36.259, 41.375, and 43,298 correspond to a cubic lattice of silver oxide reflection planes, (101), (110), (002), (102), and (201), respectively, which match with the center of cubic phase for AgNPs (JCPDS No. 96-710-9247). AgNPs' particle size was determined and calculated according to the Scherrer formula, with about 58 nm average diameter. There was no indication that other substances, including silver chloride, would have interfered with the chemical reaction; the outcome of this experiment shows that the reaction exclusively reduced AgNPs nanocrystals using the aqueous extraction of *P. census* L. Analysis of the nanoparticle crystalline structure was performed using XRD. For the measurements, a small amount of dried powder was glued to the nylon loop using highly viscous oil and placed in the center of the XRD goniometer. The registered diffractograms are shown in Fig. 5. Qualitative analysis of the diffraction patterns allowed us to state that as a result of the conducted reaction, AgNPs were formed. Using too much $AgNO_3$ in the response causes the appearance of silver chloride, the reducing agent in the plant extract. Thus, not all silver ions were able to be reduced during synthesis. In addition, many fruits and vegetables contain sodium chloride (US Food and Drug Administration, 2006). As (Mehta et al., 2017) reported, XRD analysis of synthesized NPs led to the identification of diffraction peaks originating from two crystallographic systems: metallic silver and silver chloride; the silver diffraction peaks are located on two theta axes in positions 17.27; 19.97; 28.39, 33.42, which corresponds to the planes hkl according to the Miller nomenclature: (111), (200), (220), (311). The silver chloride diffraction peaks were identified at angle values: 12.83, 14.53, 21.02; 24.71, 25.83; 33.56, which corresponds to the following planes hkl: (111), (200), (220), (311), (222), (420) (Wasilewska et al., 2023). The evaluation of the average crystallite size of nanoparticles synthesized in the presence of plant extracts

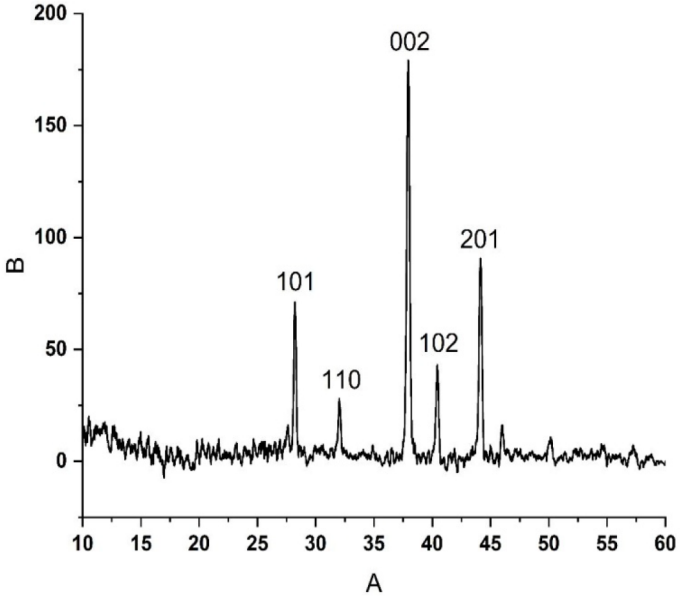

Fig. 5: X-ray diffraction (XRD) patterns of AgNPs.

was determined based on matching diffraction data with theoretical patterns of the Williamson-Hall equation (AHMAD et al., 2020). The formed nanoparticles show the highest percentage of metallic silver in the presence of apple and orange extract, which proves the complete reduction of silver ions nanostructures during synthesis. However, the highest share of silver chloride was identified in nanoparticles formed with potato, onion, and radish extracts. On the basis of collected data, it can be concluded that the factor that influences the precipitation of silver chloride may depend on the pH of the used extracts (WASILEWSKA et al., 2023). SEM. demonstrated the relatively homogeneous distribution of nanoparticles on the fracture. SEM. examined the resulting nanocomposite film surface and cross-section morphologies, moreover, Fig. 6 (A, B, C, D, E and F) displays the micrographs for each (AgNPs, starch film, nanocomposite film with 1% AgNPs, 2% AgNPs, 3% AgNPs, and 4% AgNPs respectively). According to the previous author's observations (CHENG et al., 2021; WU et al., 2023) and as can be seen from the surface photos, the starch film has a relatively flat surface as presented at Fig. 6 (B). Conversely, adding AgNPs in four different concentrations in the starch-Ag nanocomposite films caused surface roughness to increase slightly by raising the AgNPs content. However, starch-Ag nanocomposite film contained 4% AgNPs, indicating an optimal distribution of AgNPs across every nanocomposite. Moreover, the film s surface lacked any discernible holes or cracks, indicating that AgNPs had been incorporated into the starch matrix (ALMEIDA et al., 2023), glycerol, as shown in Fig. 6. Surface morphology: The Fe-SEM micrographs used to evaluate the surface morphologies of the nanocomposite films (BAGC) surface were slightly rough, with CN aggregates of 50-150 nm diameter within the polymer matrix. This indicated specific interactions among the CNs, mostly attributed to strong hydrogen bonding between the cellulose-surface hydroxyl groups (ORSUWAN, 2023).

Moisture content

The moisture content of the blend films was calculated by monitoring the weight loss of preconditioned edible films after drying in an oven at 105±1 °C for 24 h. As shown in Fig. 8 (a), the results demonstrated that the nanocomposite film contains 1, 2, 3, and 4% AgNPs, and the starch thin film lost 23.23, 21.95, 21.58, 18.83, and 23.49% of its weight, respectively.

$$MC = \frac{M1 - M2}{M1} \times 100$$

M1 is the weight of the preconditioned film sample, and M2 is the weight of the dry film sample

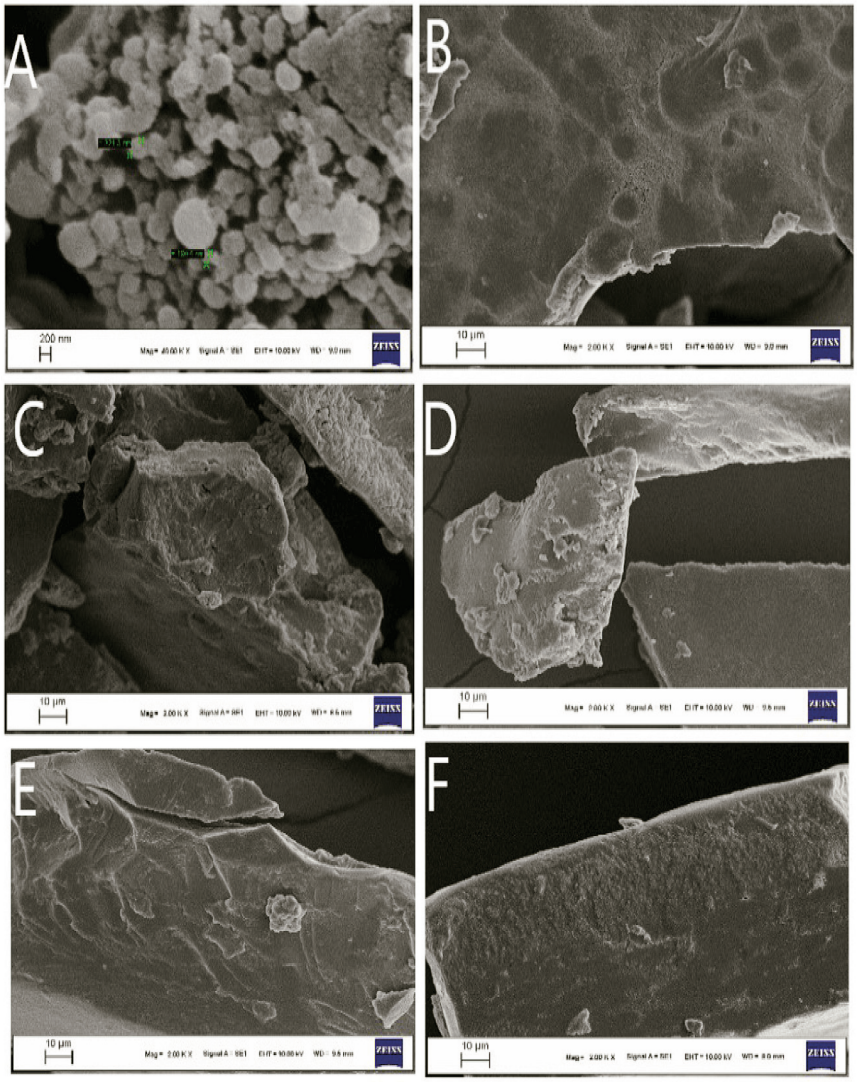

Fig. 6: **(A, B, C, D, E** and **F)** SEM Scanning Electron Microscope morphology for (AgNPs, starch film, starch-Ag nanocomposite films with 1% AgNPs, 2% AgNPs, 3% AgNPs, and 4% AgNPs respectively).

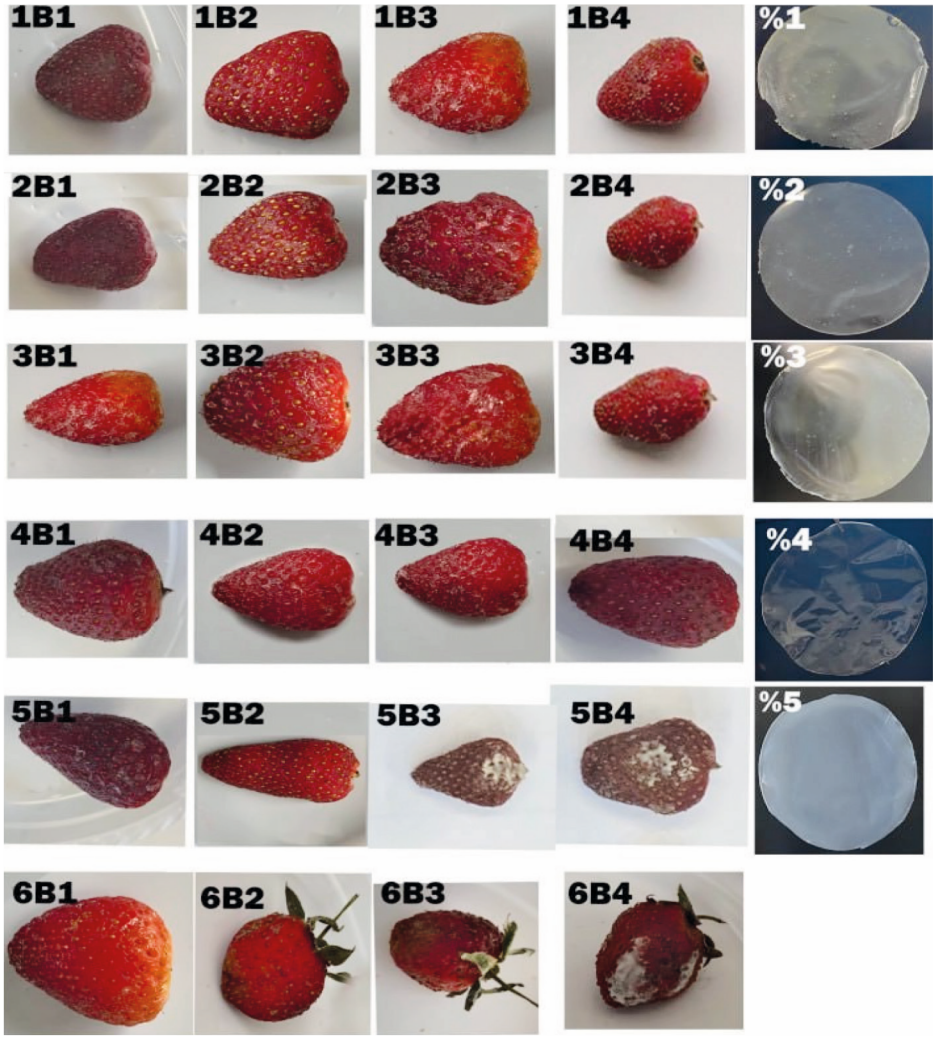

Fig. 7: Coated Strawberry fruits during storage time.
B: Strawberry fruits,
(1B1, 1B2, 1B3, and 1B4 means strawberries were coated by starch Ag-nanocomposite film containing 1% AgNPs after zero-time (first day of coating), 72 h, 1 week, 14 d, respectively).
(2B1, 2B2, 2B3, and 2B4 means strawberries were coated by starch Ag-nanocomposite film containing 2% AgNPs after zero-time (first day of coating), 72 h, 1 week, 14 d, respectively).
(3B1, 3B2, 3B3, and 3B4 means strawberries were coated by starch Ag-nanocomposite film containing 3% AgNPs after zero-time (first day of coating), 72 h, 1 week, 14 d, respectively).
(4B1, 4B2, 4B3, and 4B4 means strawberries were coated by starch Ag-nanocomposite film containing 4% AgNPs after zero-time (first day of coating), 72 h, 1 week, 14 d, respectively).
(5B1, 5B2, 5B3, and 5B4 means the starch film coated strawberries without AgNPs after zero-time (first day of coating), 72 h, 1 week, 14 d, respectively).
(6B1, 6B2, 6B3, and 6B4 means untreated strawberries after zero-time (first day of coating), 72 h, 1 week, 14 d respectively)

Adding glycerol to the film-forming fluid greatly reduced the moisture content of edible films. This may be due to the hydrophobic glycerol forming and filling hydrophobic regions in the matrix of the film. As a result, the hydrogen bonding between starch and may be decreased. Lowering the ability of the film to hold water is similar to PHUONG et al. (2023), who added tea seed oil to the chitosan edible film. As mentioned by (ORSUWAN, 2023), the addition of hydrophobic nanofiller (AgNPs) on the film surface resulted in a considerable reduction in moisture content. However, this was most likely owing to the reduced concentration of adsorbed water molecules on the banana flour/agar nanocomposite (BANC) and banana flour/agar green nanocomposite (BAGN) films compared to the neat banana flour/agar blend (BAB) and banana flour/agar green composite (BAGC).

Thickness

Each blend film sample's thickness, as shown in Fig. 8 (b), was measured at ten random locations using a digital micrometer (Chinas Qlr digit-IP54), with a 0.001 mm precision. The findings demonstrate that the thickness of nanocomposite films comprising 1, 2, 3, and 4% AgNPs and starch nanocomposite rose significantly with the increasing level of starch, measured as 0.25, 0.22, 0.20, 0.18, and 0.35 mm, respectively. This rise in thickness may be related to an increase in the films solids content. Contrarily, AgNPs cause a reduction in the thickness of the bled film when added to the composite, resulting in starch-Ag nanocomposite film with the highest amount of starch content, and the lowest amount of AgNPs having a thickest layer. This interaction reduces the alignment of the polymer chain, which limits the compression and packing of the film network and raises the film thickness (PHUONG et al., 2023).

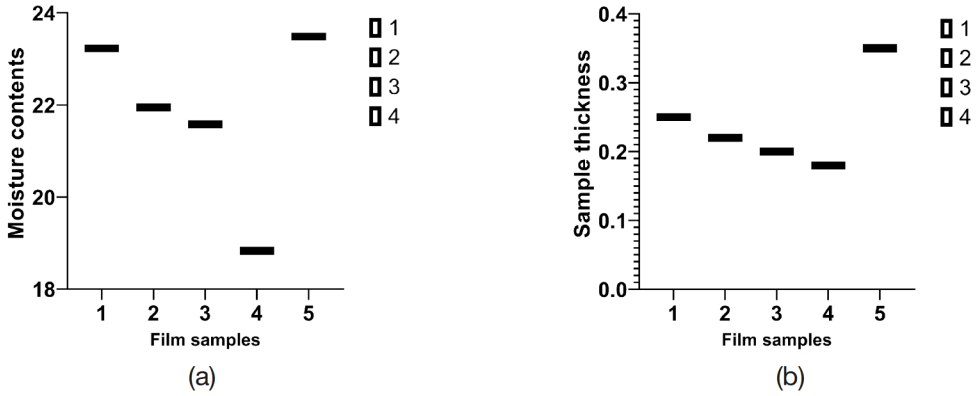

Fig. 8: **(a)** Determining film moisture content to the five different concentrations of the starch-Ag-nanocomposite films. **(b)** Determining film thicknesses to the five di ferent concentrations of the starch-Ag-nanocomposite films

Incorporating the cellulose nanocrystals (CN) and AgNPs enhanced the film thickness compared to neat banana flour/agar blend (BAB) film, owing to an increase in the solid content of the solution. The higher film thickness also reflects the roughness of the banana flour/agar green composite (BAGC) and banana flour/agar green nanocomposite (BAGN) films, as shown in the FE-SEM micrographs (ORSUWAN, 2023).

Color parameters

The colorimetric results in Fig. 9 demonstrate that the incorporation of AgNPs significantly impacts the color parameters of the starch-Ag films. In contrast, adding starch does not affect the color of the resulting starch-Ag nanocomposite films. The brightness parameter L* decreases as the level of AgNPs increases as shown in Fig. 9 (a). Also, as AgNPs content increased, a* and b* parameters were enhanced as presented in Fig. 9 (b) and (c). Additionally, the overall color difference (of the starch-Ag nanocomposite films was boosted with a greater percentage of AgNPs as shown in Fig. 9 (d). This observation agrees with those reported by ROY et al. (2019) for the agar-based film. The presence and concentration of AgNPs significantly ($p < 0.01$) affected chromaticity parameters (a* and b*). However, the corresponding values were quite low, and the nanocomposite films remained colorless. The increase in the b* parameter might be related to the chemical browning reaction of maltose in the matrix, which acts as a reducing agent during AgNPs production. A clear trend of increasing AgNPs content was not seen,

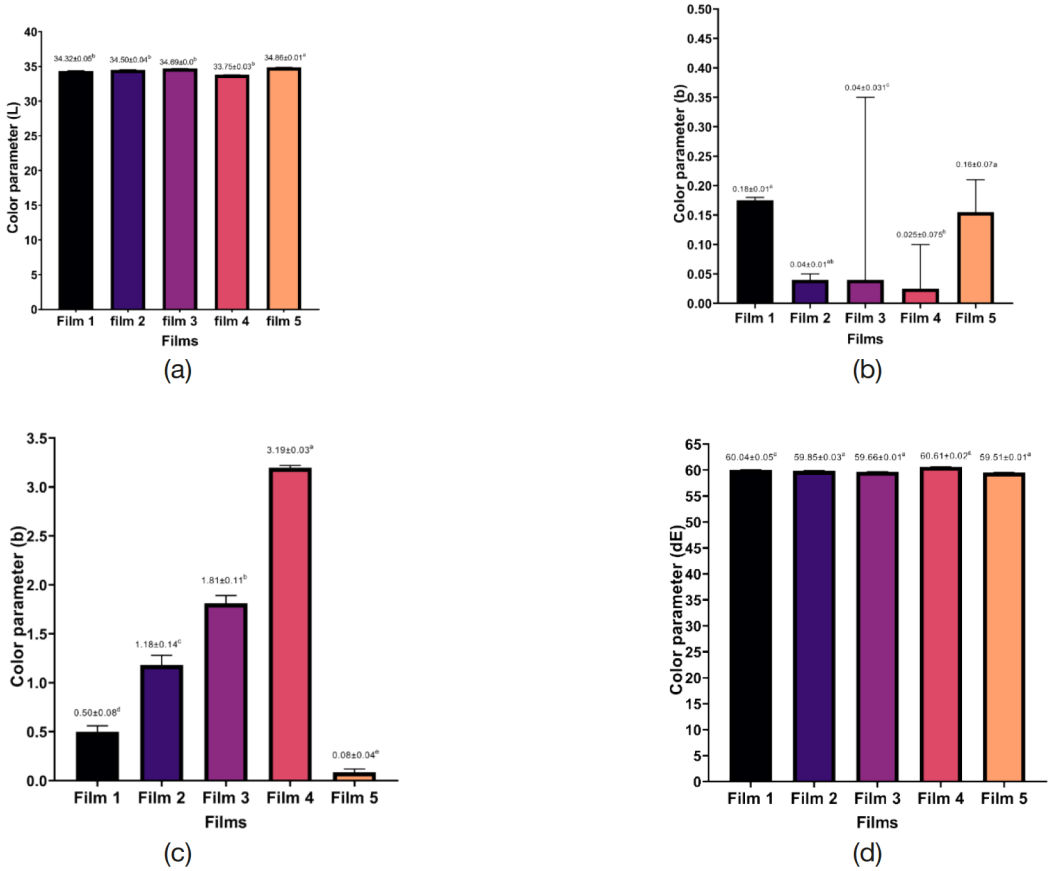

Fig. 9: **(a)** Determining (L*) color parameters for the five different concentrations of the starch-Ag-nanocomposite films. **(b)** Determining (a*) color parameters for the five different concentrations of the starch-Ag-nanocomposite films. **(c)** Determining (b*) color parameters for the five different concentrations of the starch-Ag-nanocomposite films. **(d)** Determining (DE*) color parameters for the five different concentrations of the starch-Ag-nanocomposite films

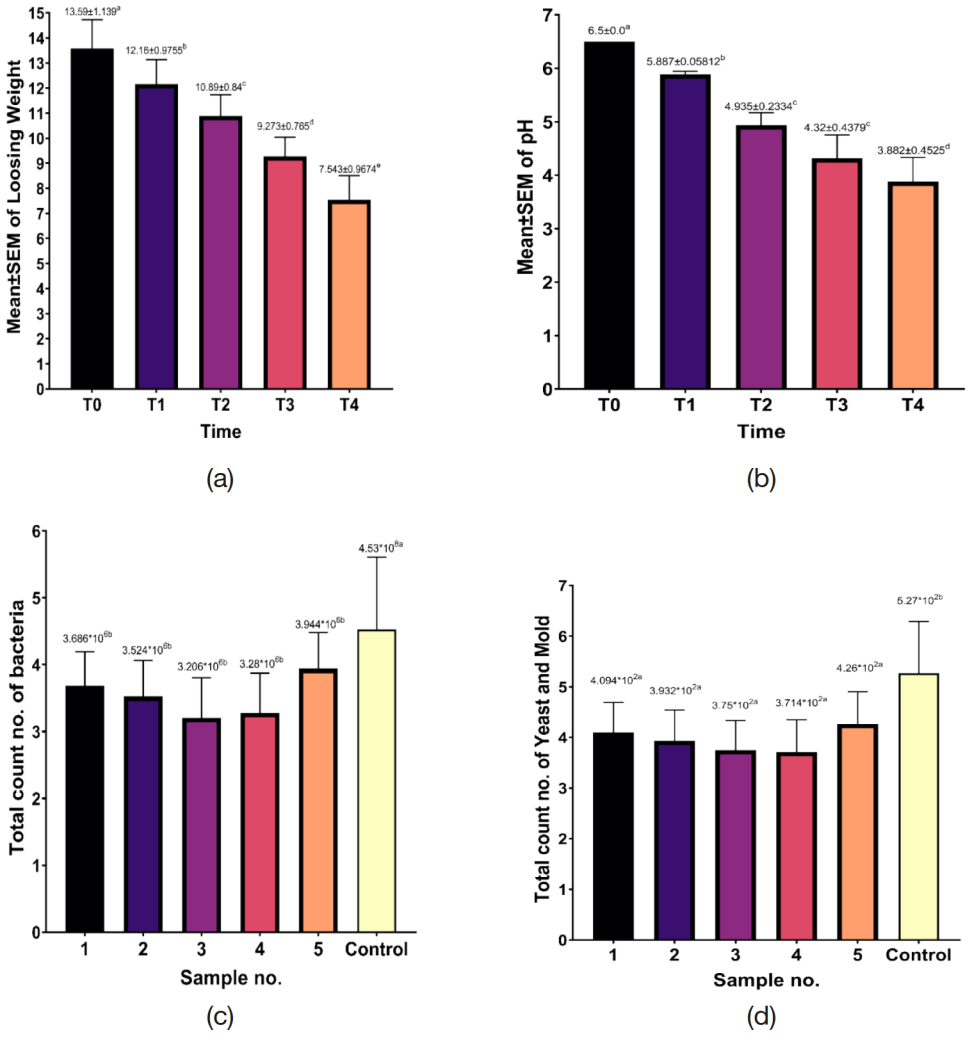

Fig. 10: **(a)** Weight losing to the five different concentrations of the starch-Ag-nanocomposite films with control during storage time. **(b)** Effect of the pH to the five different concentrations of the starch-Ag-nanocomposite films with control during storage time. **(c)** Total count number of bacteria in the coated samples with five different concentrations of the starch-Ag-nanocomposite films during storage time. **(d)** Total count number of yeast and mold in the coated samples with five di ferent concentrations of the starch-Ag-nanocomposite films during storage time
The tests of sample No. (1, 2, 3, 4, and 5) show that fruits coated with starch-Ag nanocomposite contain 1, 2, 3, and 4% AgNPs, respectively, and 5 is starch nanocomposite. The control shows untreated fruit during storage time (T0, T1, T2, T3, and T4 mean storage in zero time, 72 h, seven days, ten days, and 14 days, respectively).

most likely due to the lower dosage used in this investigation. Abreu et al. (2015) and Cheviron et al. (2014) discovered a significant rise in the b parameter, resulting in a shift from milt clear to yellow/orange color for nanocomposite films with concentrations of up to 1 mM. The addition of NPs had a substantial impact ($p < 0.01$) on luminosity (L*), with a decrease as concentration rose. The integration and concentration of AgNPs had a significant ($p < 0.01$) influence on the color difference (DE), as illustrated in Fig. 9 (d). Again, the low values suggest that the created films are practically colorless, which corresponds with cinema visual observations (Ortega et al., 2017).

Antimicrobial activity of AgNPs and starch thin film

The investigation results find that AgNPs have a potent antibacterial action in the fight against foodborne diseases. The inhibitory effects of the AgNPs samples illustrated against Gram-positive (*S. aureus*) and Gram-negative (*E. coli*) bacteria, and (*C. albicans*) as fungal micro-organisms. The AgNPs, on the other hand, showed significan antimicrobial activity. *E. coli* had the most growth inhibition at 21 ± 0.4 mm, while *S. aureus*, a Gram-positive bacteria, had the lowest growth inhibition at 18.5 ± 1.20 mm, but *C. albicans* had the highest at 12.0 ± 2.0 mm. The particle size of the AgNPs produced also affected antibacterial activity or bacterial growth inhibition. Small particles with a high surface area were picked up by the cell membrane of bacteria and interacted with them by releasing toxins. The liberated Ag ions expedited the generation of oxidative species, which are more responsible for cell membrane damage and, thus, cell death (Mohseni et al., 2020). Among the different concentrations of AgNPs in composite films, the 4% AgNPs composite film demonstrated the zone of highest inhibition (23.43 ± 2.05, 20.65 ± 1.74, and 15.82 ± 1.23 mm for *S. aureus*, *E. coli*, and *C. albicans*, respectively) as presented in Tab. 1. Previous research examined the antibacterial activity against *S. aureus* and *E. coli*. AgNPs produced a result of 15.4 ± 0.6 for *E. coli*, which was quite effective against this strain. The standard cultured value for *E. coli* was established at 37.3 ± 0.6. The results for *S. aureus* with AgNPs were 9.9 ± 1.2, compared to the typical value of 31.3 ± 1.1 (Ali et al., 2022).

In the structure of the pathogen, the accumulation of nanoparticles causes cell membrane denaturation, which may affect analyzed nano-structures' antibacterial potential. The nanoparticles showed lower

Tab. 1: Diameters of inhibition zone of Gram-negative, Gram-positive bacteria and fungi (mm)

	Antimicrobial activities of Starch-Ag composite films (mm)		
Films	***E. coli***	***S. aureus***	***C. albicans***
1%	15	18	11
2%	17	20	13
3%	18	21	14
4%	20	23	15
Starch Nanocomposite	14	18	10

Values are mean ± SD of three replicates.

activity against Gram-negative bacteria such as *E. coli*. Therefore, Gram-positive bacteria, such as *S. aureus*, are more susceptible to the harmful effects of AgNPs and have a thicker peptidoglycan layer, susceptible when compared with Gram-negative bacteria (Rhim et al., 2013; Amalraj et al., 2020; Biswas et al., 2022; Orsuwan, 2023; Wasilewska et al., 2023; Yang et al., 2023). AgNPs exhibit more cell penetration and storage antibacterial effects than silver ions (Cheng et al., 2021).

Antioxidant activity of AgNPs and starch thin film by DPPH

The antioxidant activity of both generated AgNPs and Starch-Ag nanocomposite film was evaluated using the DPPH test. AgNPs had lesser antioxidant activity than starch-Ag nanocomposites. The scavenging activity (%) of AgNPs elevated from 14 to 84%, whereas starch-Ag nanocomposites increased from 3.8 to 90.7%. The data presented above demonstrated a high antioxidant capacity against ascorbic acid. They showed that adding silver nanoparticles to the starch nanocomposite coatings could be a novel antioxidant for food processing. The following formula was used to calculate the percentage of activity for scavenging DPPH radicals (Shumi et al., 2023):

The radical form of DPPH is changed into the non-radical form, causing the color to change from violet to pale yellow DPPH is an astable free radical that binds to species that come into contact within (often the species that may transfer the electrons) and absorbs their free electrons, or hydrogen. When DPPH is exposed to AgNPs, which have the potential to transfer electrons, DPPH becomes decolored as a result of the radical scavenging that occurs. The absorbance of the DPPH radical drops over time, indicating a decrease in concentration caused by the conversion of non-radical forms or scavenging activity, an effective antioxidant feature. The results demonstrated that maximum radical scavenging (90.7%) was achieved in about 20 min for AgNPs in a starch-Ag nanocomposite film containing 3 and 4% AgNPs, demonstrating AgNP's effective antioxidant ability. The calculated time vs. percent inhibition displays the linear relationship (an ideal activity) for AgNP antioxidant capability in the DPPH assay. In addition to this, DPPH has several limitations, including the need for incubation in the dark due to light sensitivity in the scavenging process and sensitivity to the Lewis base (Ali et al., 2022). The antioxidant levels of the optimized extract with and without nanoparticles were reported by Herrera-Marín et al. (2023) to be 0.7 ± 0.1 ppm and 0.65 ± 0.05 ppm, respectively.

Nanocomposite coating

The advancements of (bio-nanocomposites) in "edible coating" with an emphasis on "strawberry preservation" will be discussed in this part, even though numerous studies have focused on diverse food packaging nano systems. Coating is frequently employed as an active packaging solution to maintain the freshness of fresh items and lengthen their shelf life (Qu and Luo, 2021). Compared to larger systems, "nanomaterials" can impart various features due to their small size. By releasing during storage times, hydrophilic or lipophilic components can be added to modern packaging technologies to boost the system's bioactivities, such as antibacterial and antioxidant.

Storage analysis for the coated foods

Due to their nutritional significance, starch-Ag nanocomposite edible films for berries like strawberries include a wide spectrum of minerals and vitamins. Strawberries, however, have limited shelf life due to high metabolic activity, sensitivity to contamination, fungal deterioration, and thin epidermis. Strawberries require the right to use technology to keep them fresh and extend their shelf life because they are expensive luxury fruits and high-value goods (Jafarzadeh et al., 2021), as presented in Fig. 7. In this investigation of the changes in gas, mechanical, and qualitative characteristics of strawberries stored using nanocomposite films made of starch, polyethylene glycol, and glycerol. When combined with silver nanoparticles, the starch-Ag nanocomposite coating sample enhanced the strawberry's physical, chemical, and mechanical qualities during storage (Jafarzadeh et al., 2021; Wigati et al., 2023).

Weight loss

Weight losses during strawberry coating can be impacted by a variety of factors, including the coating substance employed, the application technique, storage conditions, and the inherent properties of the strawberries. When strawberries are coated with a variety of edible coatings, such as polysaccharide-based coatings (e.g., starch, chitosan), the weight loss may vary depending on the coating materials, thickness, storage conditions, and strawberry characteristics. However, well-designed coverings can help to reduce weight loss when compared to untreated strawberries (Taha et al., 2022). Fig. 10 (a) shows the significant increase in weight loss during storage time. After 72 h of storage, the untreated samples lost 11.13% of their initial weight. In contrast, coated samples with starch-Ag nanocomposite at 1, 2, 3, and 4% of AgNPs, and starch nanocomposite lost 3.98, 12.8, 7.88, 11.02, and 14.98% of their initial weight, respectively. After seven days of coating, the uncoated samples lost 30.32% of their weight, whereas the strawberries coated with starch-Ag nanocomposite 1, 2, 3, 4%, and starch composite lost 12.4, 21.46, 18.33, 14.23, and 19.63%, respectively. Regarding the impact of 4 °C storage, coating techniques significantly reduced loss in weight for treated strawberries compared to uncoated samples. Up to day 14 of storage, there was no discernible difference in weight loss across coated strawberry samples. Uncoated strawberries lost the most weight during the last few days of storage (65.74%), while samples coated with starch-Ag nanocomposite at 1, 2, 3, and 4%, and starch nanocomposite alone lost 31.5, 46.7, 45.7, 46.18, and 30.12% of their weight, respectively. Application of starch-Ag nanocomposite edible film showed a significant impact ($p<0.005$) on the percentage of weight lost with 3% AgNPs causing a significantly ($p<0.005$) higher reduction compared with 1, 2, and 4% starch-Ag nanocomposite contains AgNPs and starch film alone. Among the coatings, AgNPs 3% coating had the best Effect on delaying the weight loss of strawberry samples to 14 d of storage, as shown in Fig. 10 (a). The highest losses occurred in control samples. The results were broadly in line with earlier research that showed that coatings may have prevented weight loss by acting as semi-permeable water and gas barriers that inhibit oxidative processes, respiration, and moisture loss (Gol et al., 2013; Jafarzadeh et al., 2021).

Effect of pH

The pH of strawberry coatings can have a major influence on their performance and properties when stored. Polysaccharide-based

coatings, such as starch, chitosan, or alginate, perform better at slightly acidic pH levels, improving film formation and adhesion to the strawberry surface. Maintaining the correct pH range for the coating ingredient may aid in creating a stable and continuous coating on strawberries. The pH of the coating affects its moisture barrier qualities, which are crucial in minimizing weight loss while coating strawberries. (Abera et al., 2024) reported that, the pH of coated and uncoated strawberries differs significantly ($p<0.05$). The acidity of uncoated strawberry was significantly increased compared to the coated and $p<0.05$, indicating that coating slows down changes in the pH of the fruit. The pH change of strawberries shows a significant difference for coating treatments during storage time ($p<0.005$), as presented in Fig. 10 (b). According to the study, fruit senescence and enzymatic activity may be to blame for the increase in pH during shelf life. Depending on the cultivar, ripening stage, storage circumstances, and microbial contamination, the pH of fresh strawberries is typically between 3 and 3.9. Strawberries had ultimate pH values that were relatively low after 14 d of storage in all treatments, whether uncoated or coated, which may be related to the fruit's ascorbic content.

This study showed that fruits have a lower pH due to relatively high levels of ascorbic acid. The consumption during respiration since four out of five measurements 0, 3, 7, 10, and 14 d with coated fruits utilizing the starch-Ag nanocomposite formulation had the highest pH compared with other samples. Uncoated strawberries showed a difference as early as day 3. On day 10, the pH content of uncoated fruit was 2.4. In contrast, the pH content of samples coated with starch-Ag nanocomposite at 1, 2, 3, and 4% AgNPs and starch nanocomposite mg L1 was 5, 4.6, 5.1, 5.1, and 3.7, respectively, as shown in Fig. 10 (b). The pH of uncoated fruit reached two on day 14 of storage. The pH content of uncoated fruit reached 2. In contrast, the pH of samples coated with starch-Ag nanocomposite at 1, 2, 3, and 4% AgNPs and starch nanocomposite mg L1 reached 4.7, 4.1, 4.5, 4.8, and 3.1, respectively, whereas the untreated sample was rejected. The sample coated with starch-Ag nanocomposite mg L1 had the least decline at the end of storage at cold storage (day 14). In the physiological and metabolic activities of fruit, fruit respiration, and acid consumption can be slowed down by nanocoating. As a result, the nanomembrane extends strawberry shelf life.

Changes in microbial load for strawberry fruit during storage

As seen in Fig. 10 (c), the total bacterial count decreased when the coating was applied. It should be noted that all samples' initial T.B.C. rose during storage, particularly in untreated fruits, which accelerated more quickly than in other samples. After 72 hrs of storage at 4 °C, the starting amounts of T.B.C. grew to 4.63 log CFU/g for the untreated sample, compared to 2.84, 2.68, 2.53, 2.61, and 3.12 log CFU/g for the samples treated with starch-Ag nanocomposite contain AgNPs 1, 2, 3, and 4%, and starch film respectively. Fruit coated with starch-Ag nanocomposite 3% AgNPs exhibited the lowest bacterial count (2.01 log CFU/g) of fruits coated with starch film (3.65 log CFU/g) on day 7 of storage. In contrast, fruit covered in Starch-Ag nanocomposite 3% AgNPs exhibited bacterial count of about (5.08 log CFU/g) of fruits were coated with starch film on day 14 of storage. Coated samples with starch film increased by 5.27 log CFU/g, although untreated samples were rejected at day 14 of storage, demonstrating the performance of coating in growth inhibition of bacteria. According to the findings, the coating in strawberry fruits was more effective than the control in controlling T.B.C. On the other hand, AgNPs can significantly inhibit growing bacteria in fruits. Fig. 10 (d) also shows the mold and yeast level variations in coated and uncoated strawberries over time. Initial concentrations of mold and yeast in fresh fruit were 2.25 log CFU/g; however, the levels of mold and yeast were reduced to 3.5, 3.1, 2.92, 2.89, and 3.6 log CFU/g, respectively, immediately following 72 h of coating. These findings are consistent with those who discovered 2.11 log CFU/g for fresh strawberries' mold count and yeast. The mold and yeast counts grew in all samples after storage. The untreated samples rose more quickly and attained higher levels than the treated ones and higher levels more quickly than the covered ones. The untreated strawberry had the highest yeast and mold count (3.8 log CFU/g) after 72 h, while the starch-Ag nanocomposite 3% AgNPs coated strawberries had the lowest number of yeast and mold count (2.92 log CFU/g). In contrast, after 14 d of storage in the fridge (4 °C), fruit coated with starch-Ag nanocomposite 3% AgNPs showed decreased yeast and mold counts (5.36 log CFU/g). According to the findings observed and displayed in Fig. 10 (d), nanocoating demonstrated antimicrobial properties by preventing or delaying the formation of yeast and mold.

Conclusions

In this investigation, starch and glycerol composite films with and without silver nanoparticles synthesized from sour cherry were developed via optimization, and their structural, physical, thermal, antimicrobial, and antioxidant properties were characterized. The processed thermoplastic starch-Ag nanocomposite films exhibited a rougher surface with more protrusions, as morphological studies of increasing AgNPs showed. The development of intermolecular interactions, such as hydrogen bonds, between the film s constituent molecules was validated by FTIR analysis. As a result, adding AgNPs may enhance the starch-Ag composite films mechanical, barrier, and water resistance qualities. Above all, when the amount of AgNPs increased, the composite films demonstrated outstanding DPPH radical scavenging properties. In addition, all the developed starch-Ag nanocomposite films possessed good antimicrobial activity, and starch-Ag films could significantly slow down the oxidative deterioration of strawberry fruits during storage. Thus, thermoplastic processed Starch-Ag films incorporating fresh strawberry fruits extend their shelf life to 14 d, containing articles.

Conflict of interest

No potential conflict of interest was reported by the authors

References

Ahmad, S.A., Das, S.S., Khatoon, A., Ansari, M.T., Afzal, M., Hasnain, M.S., Nayak, A.K., 2020: Bactericidal activity of silver nanoparticles: A mechanistic review. Mat Sci Energy Technol, 3, 756-769. DOI: 10.1016/j.mset.2020.09.002

Alam, M., 2022: Analyses of biosynthesized silver nanoparticles produced from strawberry fruit pomace extracts regarding biocompatibility, cytotoxicity, antioxidant ability, photodegradation, and in-silico studies. J. King Saud University-Sci., 34, 102327. DOI: 10.1016/j.jksus.2022.102327

Ali, F., Younas, U., Nazir, A., Hassan, F., Iqbal, M., Mukhtar, S., Khalid, A., Ishfaq, A., 2022: Biosynthesis and characterization of silver nanoparticles using strawberry seed extract and evaluating their antibacterial and antioxidant activities. J. Saudi Chem. Soc. 26, 101558. DOI: 10.1016/j.jscs.2022.101558

Almeida, T., Karamysheva, A., Valente, B.F., Silva, J.M., Braz, M., Almeida, A., Silvestre, A.J., Vilela, C., Freire, C.S., 2023: Biobased ternary films of thermoplastic starch, bacterial nanocellulose, and gallic acid for active food packaging. Food Hydrocoll. 144, 108934. DOI: 10.1016/j.foodhyd.2023.108934

Amalraj, A., Haponiuk, J.T., Thomas, S., Gopi, S., 2020: Preparation, characterization, and antimicrobial activity of polyvinyl alcohol/gum arabic/chitosan composite films incorporated with black pepper essential oil and ginger essential oil. Int. J. Biol. Macromol. 151, 366-375. DOI: 10.1016/j.ijbiomac.2020.02.176

Arrieta, M.P., Peltzer, M.A., Del Carmen Garrigós, M., Jiménez, A., 2013: Structure and mechanical properties of sodium and calcium

caseinate edible active films with carvacrol. J. Food Eng. 14, 486-494. DOI: 10.1016/j.jfoodeng.2012.09.002

Başyiğit, B., Sağlam, H., Kandemir, Ş., Karaaslan, A., Karaaslan, M., 2020: Microencapsulation of sour cherry oil by spray drying: Evaluation of physical morphology, thermal properties, storage stability, and antimicrobial activity. Powder Technol. 364, 654-663. DOI: 10.1016/j.powtec.2020.02.035

Başyiğit, B., Yücetepe, M., Akyar, G., Karaaslan, A., Karaaslan, M., 2022: Enhancing thermal and emulsifying resilience of pomegranate fruit protein with gum Arabic conjugation. Colloids and Surfaces B: Biointerfaces, 215, 112516. DOI: 10.1016/j.colsurfb.2022.112516

Biswas, R., Alam, M., Sarkar, A., Haque, M.I., Hasan, M.M., Hoque, M., 2022: Application of nanotechnology in food: Processing, preservation, packaging, and safety assessment. Heliyon 8 (11). DOI: 10.1016/j.heliyon.2022.e11795

Cheng, J., Lin, X., Wu, X., Liu, Q., Wan, S., Zhang, Y., 2021: Preparation of a multifunctional silver nanoparticles polylactic acid food packaging film using mango peel extract. Int. J. Biol. Macromol. 188, 678-688. DOI: 10.1016/j.ijbiomac.2021.07.161

De Matteis, V., Cascione, M., Costa, D., Martano, S., Manno, D., Cannavale, A., Mazzotta, S., Paladini, F., Martino, M., Rinaldi, R., 2023: *Aloe vera* silver nanoparticles addition in chitosan films: improvement of physicochemical properties for eco-friendly food packaging material. J. Mat. Res. Technol. 24, 1015-1033. DOI: 10.1016/j.jmrt.2023.03.025

Demirbas, A., BüYüKbezirci, K., Celik, C., Kislakci, E., Karaagac, Z., Gokturk, E., Kati, A., Cimen, B., Yilmaz, V., Ocsoy, I., 2019: Synthesis of long-term stable gold nanoparticles benefiting from red raspberry (*Rubus idaeus*), strawberry (*Fragaria ananassa*), and blackberry (*Rubus fruticosus*) extracts–gold ion complexation and investigation of reaction conditions. ACS omega, 4, 18637-18644. DOI: 10.1021/acsomega.9b02469

Donno, D., Cavanna, M., Beccaro, G.L., Mellano, M.G., Torello Marinoni, D., Cerutti, A.K., Bounous, G., 2013: Currants and strawberries as bioactive compound sources: Determination of antioxidant profiles with HPLC-DAD/MS. J. Appl. Bot. Food. Qual. 86, 1-10. DOI: 10.5073/JABFQ.2013.086.001

Duncan, T.V., 2011: Nanotechnology applications in food packaging and safety include barrier materials, antimicrobials, and sensors. J. Colloid Interface Sci., 363, 1-24. DOI: 10.1016/j.jcis.2011.07.017

Ekrikaya, S., Yilmaz, E., Celik, C., Demirbuga, S., Ildiz, N., Demirbas, A., Ocsoy, I., 2021. Investigation of ellagic acid rich-berry extracts directed silver nanoparticles synthesis and their antimicrobial properties with potential mechanisms towards *Enterococcus faecalis* and *Candida albicans*. J. Biotechnol. 341, 155-162. DOI: 10.1016/j.jbiotec.2021.09.020

Farnsworth, N.R., 1966: Biological and phytochemical screening of plants. J. Pharmaceut. Sci. 55, 225-276. DOI: 10.1002/jps.2600550302

Ferdous, Z., Nemmar, A., 2020: Health impact of silver nanoparticles: a review of the biodistribution and toxicity following various routes of exposure. Int. J. Mol. Sci. 21, 2375. DOI: 10.3390%2Fijms21072375

Fonseca, L.R., Silva, G.R., Luís, Â., Cardoso, H.J., Correia, S., Vaz, C.V., Duarte, A.P., Socorro, S., 2021: Sweet cherries as anti-cancer agents: From bioactive compounds to function. Molecules 26, 2941. DOI: 10.3390/molecules26102941

Gol, N.B., Patel, P.R., Rao, T.R., 2013: Improvement of quality and shelf life with edible coatings enriched with chitosan. Postharv. Biol. Technol. 85, 185-195. DOI: 10.1016/j.postharvbio.2013.06.008

Herrera-Marín, P., Fernández, L., Pilaquinga, F., Debut, A., Rodríguez, A., Espinoza-Montero, P., 2023: Green synthesis of silver nanoparticles using aqueous extract of the leaves of fine aroma cocoa *Theobroma cacao* line (Malvaceae): Optimization by electrochemical techniques. Electrochim. Acta 447, 142122. DOI: 10.1016/j.electacta.2023.142122

Hurtado-Barroso, S., Trius-Soler, M., Lamuela-Raventós, R.M., Zamora-Ros, R., 2020: Vegetable and fruit consumption and prognosis among cancer survivors: a systematic review and meta-analysis of cohort studies. Adv. Nutr. 11, 1569-1582. DOI: 10.1093/advances/nmaa082

Jafarzadeh, S., Nafchi, A.M., Salehabadi, A., Oladzad-Abbasabadi, N., Jafari, S.M., 2021: Application of bio-nanocomposite films and edible coatings for extending the shelf life of fresh fruits and vegetables. Adv. Colloid Interface Sci. 291, 102405. DOI: 10.1016/j.cis.2021.102405

Khoo, H.E., Azlan, A., Tang, S.T., Lim, S.M., 2017: Anthocyanidins and anthocyanins: Colored pigments as food, pharmaceutical ingredients, and the potential health benefits. Food Nut . Res. 61, 1361779. DOI: 10.1080/16546628.2017.1361779

Kumar, R., Ghoshal, G., Goyal, M., 2020: Development and characterization of corn starch-based nanocomposite film with AgNPs and plant extract. Mat. Sci. Energy Technol. 3, 672-678. DOI: 10.1016/j.mset.2020.07.004

Mao, S., Li, F., Zhou, X., Lu, C., Zhang, T., 2023: Characterization and sustained release study of starch-based films loaded with carvacrol: A promising UV-shielding and bioactive nanocomposite film. LWT, 180, 114719. DOI: 10.1016/j.lwt.2023.114719

Mehta, B., Chhajlani, M., Shrivastava, B., 2017: Green synthesis of silver nanoparticles and their characterization by XRD. J Physics: conference series, 2017. IOP Publishing, 012050.

Mohseni, M.S., Khalilzadeh, M.A., Mohseni, M., Hargalani, F.Z., Getso, M.I., Raissi, V., Raiesi, O., 2020: Green synthesis of Ag nanoparticles from pomegranate seed extracts, synthesis of Ag-Starch nanocomposite, and characterization of mechanical properties of the films. Biocat. Agric. Biotechnol. 25, 101569. DOI: 10.1016/j.bcab.2020.101569

Omar-Aziz, M., Khodaiyan, F., Yarmand, M. S., Mousavi, M., Gharaghani, M., Kennedy, J.F., Hosseini, S.S., 2021: Combined effects of octenylsuccination and beeswax on pullulan films: Water-resistant and mechanical properties. Carbohydrate polymers, 255, 117471. DOI: 10.1016/j.carbpol.2020.117471

Orsuwan, A., 2023: Effect of cellulose nanocrystals and green synthesized silver nanoparticles on mechanical properties and antimicrobial activity of banana flour/agar composite films. Heliyon, 9 DOI: 10.1016/j.heliyon.2023.e15102

Ortega, F., Giannuzzi, L., Arce, V.B., García, M.A., 2017: Active composite starch films containing green synthesized silver nanoparticles. Food Hydrocoll. 70, 152-162. DOI: 10.1016/j.foodhyd.2017.03.036

Phuong, N.T.H., Koga, A., Nkede, F.N., Tanaka, F., Tanaka, F., 2023: Application of edible coatings composed of chitosan and tea seed oil for quality improvement of strawberries and visualization of internal structure changes using X-ray computed tomography. Prog. Organic Coat. 183, 107730. DOI: 10.1016/j.porgcoat.2023.107730

Pirsa, S., Karimi Sani, I., Pirouzifard, M.K., Erfani, A., 2020: A smart film based on chitosan/Melissa officinalis essences/pomegranate peel extract to detect cream cheese spoilage. Food Addit. Contam., Part A, 37, 634-648. DOI: 10.1080/19440049.2020.1716079

Qu, B., Luo, Y., 2021: A review of preparing and characterizing chitosan-clay nanocomposite films and coatings for food packaging applications. Carbohydr. Polymer. Technol. Applic. 2, 100102. DOI: 10.1016/j.carpta.2021.100102

Rhim, J., Wang, L., Hong, S., 2013: Preparation and characterization of agar/silver nanoparticles composite films with antimicrobial activity. Food Hydrocoll. 33, 327-335. DOI: 10.1016/j.foodhyd.2013.04.002

Roy, S., Rhim, J.-W., Jaiswal, L., 2019: Bioactive agar-based functional composite film incorporated with copper sulfide nanoparticles. Food Hydrocoll. 93, 156-166. DOI: 10.1016/j.foodhyd.2019.02.034

Sambucetti, M., Zuleta, A., 1996: Resistant starch in dietary fiber values measured by the AOAC method in different cereals. Cereal Chem. 73, 759-761.

Seekonda, S., Rani, R., 2022: Eco-friendly synthesis, characterization, catalytic, antibacterial, antidiabetic, and antioxidant activities of *Embelia robusta* seeds extract stabilized AgNPs. J. Sci. Adv. Mat. Dev. 7, 100480. DOI: 10.1016/j.jsamd.2022.100480

Shankar, S., Khodaei, D., Lacroix, M., 2021: Effect of chitosan/essential oils/silver nanoparticles composite films packaging and gamma irradia-

tion on shelf life of strawberries. Food Hydrocoll. 117, 106750. DOI: 10.1016/j.foodhyd.2021.106750

Sheikh, A.A., Wani, Z.A., Shah, A.M., Hassan, Q.P., Mondhe, D.M., Verma, M.K., 2022: Chemopreventive effects of *Prunus cerasus* L. against human cancer cells and ascites mice models and its phytochemical investigation by LC-Q-TOF-MS/MS. Phytomed. Plus, 2, 100336. DOI: 10.1016/j.phyplu.2022.100336

Shumi, G., Demissie, T.B., Eswaramoorthy, R., Bogale, R.F., Kenasa, G., Desalegn, T., 2023: Biosynthesis of Silver Nanoparticles Functionalized with Histidine and Phenylalanine Amino Acids for Potential Antioxidant and Antibacterial Activities. ACS Omega. DOI: 10.1021/acsomega.3c01910

Skiba, M.I., Vorobyova, V.I., Pivovarov, A., Makarshenko, N.P., 2020: Green synthesis of silver nanoparticles in the presence of polysaccharide: optimization and characterization. J. Nanomat. 2020, 1-10. DOI: 10.1155/2020/3051308

Suman, T., Rajasree, S.R., Kanchana, A., Elizabeth, S.B., 2013: Biosynthesis, characterization and cytotoxic effect of plant-mediated silver nanoparticles using *Morinda citrifolia* root extract. Coll. Surf. B: Biointerfaces, 106, 74-78. DOI: 10.1016/j.colsurfb.2013.01.037

Tacha, S., Somord, K., Rattanawongkun, P., Intatha, U., Tawichai, N., Soykeabkaew, N., 2023: Bio-nanocomposite foams of starch reinforced with bacterial nanocellulose fibers. Mat. Today: Proceed. 75, 119-123. DOI: 10.1016/j.matpr.2022.12.049

Taha, I.M., Zaghlool, A., Nasr, A., Nagib, A., El Azab, I.H., Mersal, G.A., Ibrahim, M.M., Fahmy, A., 2022: Impact of starch coating embedded with silver nanoparticles on strawberry storage time. Polymers 14, 1439. DOI: 10.3390/polym14071439

Teodoro, A.P., Mali, S., Romero, N., De Carvalho, G.M., 2015: Cassava starch films containing acetylated starch nanoparticles as reinforcement: Physical and mechanical characterization. Carbohydr. Polymers 126, 9-16. DOI: 10.1016/j.carbpol.2015.03.021

van De Klashorst, D., van Den Elzen, A., Weeteling, J., Roberts, M., Desai, T., Bottoms, L., HUGHES, S., 2020: Montmorency tart cherry (Prunus et al.) is a calorie restriction mimetic that increases intestinal fat and lifespan in *Caenorhabditis elegans*. J. Funct. Foods, 68, 103890. DOI: 10.1016/j.jff.2020.103890

Vinodhini, S., Vithiya, B.S.M., Prasad, T.A.A., 2022: Green synthesis of silver nanoparticles by employing the *Allium fistulosum*, *Tabernaemontana divaricate*, and *Basella alba* leaf extracts for antimicrobial applications. J. King Saud Univ.-Sci. 34, 101939. DOI: 10.1016/j.jksus.2022.101939

Wasilewska, A., Klekotka, U., Zambrzycka, M., Zambrowski, G., Święcicka, I., Kalska-Szostko, B., 2023: Physico-chemical properties and antimicrobial activity of silver nanoparticles fabricated by green synthesis. Food Chem. 400, 133960. DOI: 10.1016/j.foodchem.2022.133960

Wigati, L.P., Wardana, A.A., Tanaka, F., Tanaka, F., 2023: Strawberry preservation using yam bean starch, agarwood Aetoxylon body essential oil, and calcium propionate edible coating during cold storage evaluated by TOPSIS-Shannon entropy. Prog. Org. Coat. 175, 107347. DOI: 10.1016/j.porgcoat.2022.107347

Wu, H., Li, T., Peng, L., Wang, J., Lei, Y., Li, S., Li, Q., Yuan, X., Zhou, M., Zhang, Z., 2023: Developing and characterizing antioxidant composite films based on starch and gelatin incorporating resveratrol fabricated by extrusion compression molding. Food Hydrocoll. 139, 108509. DOI: 10.1016/j.foodhyd.2023.108509

Yang, D., Liu, Q., Gao, Y., Wan, S., Meng, F., Weng, W., Zhang, Y., 2023: Characterization of silver nanoparticles loaded chitosan/polyvinyl alcohol antibacterial films for food packaging. Food Hydrocoll. 136, 108305. DOI: 10.1016/j.foodhyd.2022.108305

Yildiz, D., Gürel, D.B., Çağindi, Ö., Kayaardi, S., 2022: Heat treatment and microwave applications on homemade sour cherry juice: The effect on anthocyanin content and some physicochemical properties. Curr. Plant Biol. 29, 100242. DOI: 10.1016/j.cpb.2022.100242

ORCID
Bülent Başyiğit https://orcid.org/0000-0002-6617-1836
Mehmet Karaaslan https://orcid.org/0000-0001-8097-9535

Address of the corresponding author:
Mehmet Karaaslan, Harran University, Engineering Faculty, Food Engineering Department, Şanlıurfa, Turkey
E-mail: mk385@cornell.edu